OPEN ACCESS

Scholars International Journal of Biochemistry
Abbreviated Key Title: Sch Int J Biochem
ISSN 2616-8650 (Print) | ISSN 2617-3476 (Online)
Scholars Middle East Publishers, Dubai, United Arab Emirates
Journal homepage: https://saudijournals.com

Original Research Article

Structural Bioinformatics Study Revealed Inhibition of Acute Myeloid Leukemia through Targeting Inhibition *BTG2* Gene by Using Herbal Medicine

Amr Hassan[1*], Sameh E. Hassanein[2, 3], Elsayed A. Elabsawy[1]

[1]Department of Bioinformatics, Genetic Engineering and Biotechnology Research Institute (GEBRI), University of Sadat City, Sadat 32897, Egypt
[2]Agricultural Genetic Engineering Research Institute (AGERI), Agriculture Research Center (ARC), Giza, Egypt
[3]Bioinformatics Program, School of Biotechnology, Nile University, Giza, Egypt

DOI: https://doi.org/10.36348/sijb.2024.v07i07.001 | **Received:** 18.08.2024 | **Accepted:** 22.09.2024 | **Published:** 11.11.2024

***Corresponding author:** Amr Hassan
Department of Bioinformatics, Genetic Engineering and Biotechnology Research Institute (GEBRI), University of Sadat City, Sadat 32897, Egypt

Abstract

Acute myeloid leukemia (AML) is responsible for more than 40% of adult patients suffering from adverse effects leading to death around the world. The B-cell translocation gene 2 (*BTG2*) gene work as a tumor suppressor. In this study, a list of medicinal herb compounds and drugs was investigated for their pharmacokinetic properties and cytotoxicity by applying the SwissADME, pkCSM, and Molsoft LLC websites. The molecular docking between the medicinal herbs and AML-standard drugs against the human *BTG2* gene was carried out by Auto-dock Vina. Furthermore, protein-protein interactions, gene ontology, and gene enrichment analysis were investigated to display the biological pathways related to *BTG2*. Also, molecular dynamics simulation was examined to study the behavior of the BTG2 protein and the protein-ligand complex. The present work exhibited that hesperidin displayed the highest binding affinity of −7.0 kcal/mol when interacting and docked against the BTG2 protein, while Cytarabinee and daunorubicin had binding affinity of 5.0 and 5.8 kcal/mol, respectively. The PPI highlighted 101 interactions with P-values less than 10 e^{-16}., and the highest similarity score of 0.13 was found in *P53* transcriptional gene network pathways. Interestingly, gene enrichment analysis illustrated that RNA degradation was the most significant enrichment pathway. Also, BTG2 contributes to the *P53* signaling pathway in chronic myeloid leukemia. Via GADD45A gene. Molecular dynamics simulations were carried out for the highest binding docking (BTG2-hesperidin) complex, and the results revealed conformational alterations with more pronounced surface residue fluctuations in BTG2. The direct interaction of hesperidin with various crucial amino-acid residues like HIS 49, CYS 67, ARG 69, ASN 71, ASP 75, ARG 112, and THR 101 causes modifications in these residues, which ultimately attenuate the activity of the BTG-2 protein. The molecular dynamics determine the four numbers of H-bonds for executing the interaction between BTG2 and hesperidin. The best residue with high energy around all poses is Arg69. Finally, the present work highlighted that hesperidin was the highest phytochemical compound binding to BTG2 protein.

Keywords: BTG2, Acute myeloid leukemia, Herbal Medicine, molecular dynamics simulation, Molecular docking.

INTRODUCTION

AML is a common cancer disease in the world [1], which is characterized by the un-regularized growth of abnormal leucocytes in the bone marrow and is effective in the process of normal blood cell production [2]. European Leukemia Net (ELN) categorized AML patients into three groups: poor, intermediate, and favorable, according to mutations in leading genes [3]. *BTG2* is included in different activities, especially in tumor cells that are severed as tumor suppressors [4]. Interestingly, the interaction between *BTG2* and miR-21 is observed in many human cells. The up-regulated of miR-21 has appeared in different cancerous cells, such as lung, gastric, and colon cancers [5]. Previous articles reported that *BTG2* can be utilized as a promising biomarker for prognosis in cancer patients due to its ability to be linked with various tumor suppressor genes like *P53*, *P73*, and *RB* [6]. Chemotherapy is the most

conventional approach to remedying AML, but it causes significant issues for patients due to its harmful effect on normal cells. Hence, the scientists focus on other approaches, such as herbal medicine, which acknowledges medicinal chemistry or phytochemical herbals [7, 8]. Hesperidin is considered a flavonoid compound that belongs to the flavanone group, which exists in citrus fruits. Hesperidin has been documented to have antitumor potential due to its ability to activate and organize many cells signaling pathways, such as apoptosis, cell cycle arrest, and cell signaling pathways [9]. Both oleuropein and ligstroside are enrichens with phenolic compounds present in Extra Virgin Olive Oil (EVOO) [10]. Previous experimental studies emphasized the efficiency of olive leaf extract, including oleuropein, in decreasing proliferation and motility in various cancer cells, such as chronic myeloid leukemia and colon carcinoma. The mechanism of action to inhibit the cancerous cell by oleuropein depends on the neutralization of the aerobic glycolysis exploited by tumor cells [11, 12]. Salidroside, or p-hydroxyphenethyl-b-D-glucoside, is the main constituent of *Rhodiola rosea* L. [13]. Post-studies studies clarified the importance of salidroside in many pharmacological activity processes, such as anti-inflammatory, anti-aging, and anti-tumor properties [14]. Also, salidroside has a crucial role in inducing apoptosis through the activation of the apoptosis-autophagy mechanism [15]. Gallic acid is present in many foods, such as gallnuts and blueberries [16]. Many documents articulated the activities of gallic acid to work as anti-metastasis, pro-apoptosis, and anti-proliferation against types of cancerous cells, especially leukemia cancer cells [17, 18]. Cinnamic acid has been well-known as an anticancer agent for decades [19].

MATERIAL AND METHODS

Bioinformatic analysis of BTG2 protein

Determine the binding sites of the target protein (BTG2)

The crystal structure of the BTG2 gene (3dju) was retrieved from the protein data bank (https://www.rcsb.org/structure/3DJU) [20]. Then, applying the FT Map Webserver (https://ftmap.bu.edu/) to evaluate the availability of all residues to form hydrogen bonds and hydrophobic interactions [21].

Gene ontology analysis

The expression patterns of every single gene in specific biological processes as well as metabolic molecular pathways. The determination and identification of molecular pathways by KEGG were carried out by using ENRICHER [22] and shinyGO [23]. The functional gene ontology is enriched and visualized. Herein, we applied the $p < 0.05$ value corrected by using the Benjamini & Hochberg algorithm, which was assigned as the suitable threshold for identifying biological processes and pathways [24]. Protein-protein interaction (PPI) was applied by using an online website (STRING v. 12.0); (http://string-db.org/, accessed on March 7, 2024) [23]. The medium confidence score was 0.4, which is considered a significant value. Protein-protein interaction was analyzed and visualized by utilizing Cytoscape software [24]. Also, we applied molecular complex detection (MCODE) to clarify and find gene clusters in the PPI [25, 26].

Ligand Preparation

The 2D structures of Hesperidin, Ligustroside, Salidroside, Oleuropein, Hesperetin, Gallic Acid, Cinnamic Acid, Cytarabinee, and Daunorubicin were retrieved from the PubChem database (PubChem CID: 10621, 14136859, 159278, 5281544, 72281, 370, 444539, 6253, and 30323) are illustrated in Figure 1. According to Rasool *et al*. (2018) [27], all the 2D were converted into 3-dimensional and the energy was minimized by applying Avogadro 1.2.0 software [28].

Molecular Docking

The target protein BTG2 (3dju) was prepared by a regular process including removing water, adding hydrogens, adding polar hydrogen, and Gasteiger charges using AutoDock Tools 4.2.6. The prepared structures were saved as PDBQT files [29]. The software AutoDock 1.5.2 was applied to do all molecular docking calculations. The main cavity point axes of BTG2 protein were (center_x: -13.296, center_y: 14.374, center_z: -9.45). The binding affinity was measured using a scoring function that was carried out by AutoDock Vina [30].

Molecular Dynamic Simulation

Molecular dynamics simulation of 100 ns was applied for the best binding score by applying GROMACS-2023.1. The CHARMM36 force field was utilized to prepare the protein topology, and the General Force Field (CGenFF) server was used to prepare the ligand topology. The system was solved in in TIP3P water box of size 12Å buffer to avoid the interaction of atoms when moving off the box edge. Ions were added using the steepest descent minimization algorithm, and sodium and chloride ions were used for protein neutralization. Energy minimization was applied to the complex to avoid steric clashes using the steepest descent minimization algorithm; the force cutoff was set to 10.0 kJ/mol, and the maximum number of steps was 50000. Next, two equilibration processes were applied: NVT and NPT equilibration using a modified Berendsen thermostat and leap-frog integrator for 50000 steps, which are equivalent to 10 ps. Finally, the MD simulation runs for 100 ns, with 2 fs at each step [30]. the data were analyzed for the RMSD, RMSF (root mean square fuctuation), hydrogen bond distribution, and Rg using VMD v1.9.3 program [31, 32].

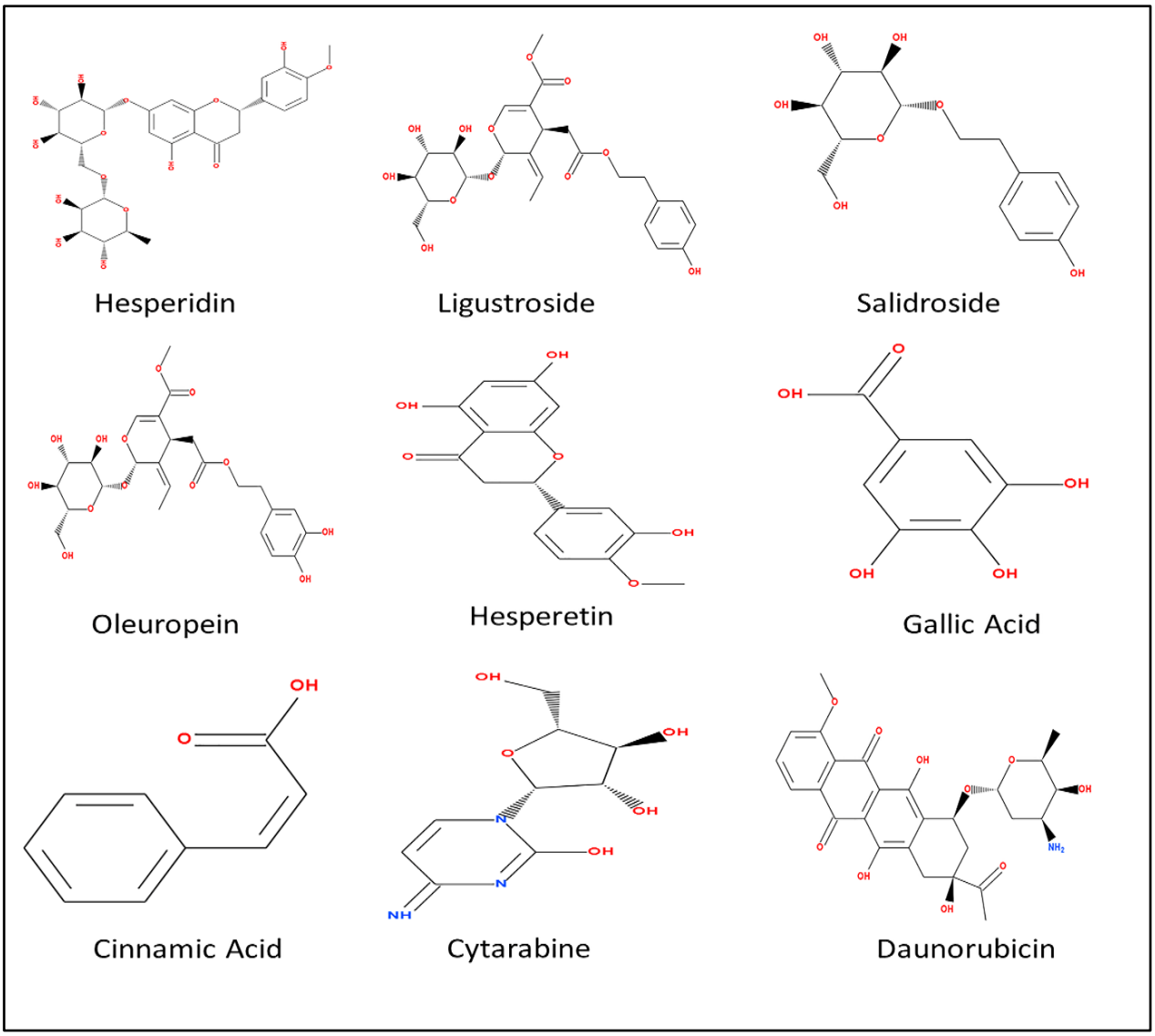

Figure 1: 2D structures of natural phytochemicals and standard drugs are used against acute myeloid leukemia (AML)

ADMET and Drug-Likeness Properties

The pharmacokinetics of Hesperidin, Ligustroside, Salidroside, Oleuropein, Hesperetin, Gallic Acid, Cinnamic Acid, Cytarabinee, and Daunorubicin were determined by utilizing the online websites SwissADME (http://www.swissadme.ch/), accessed on March 2, 2024, and pkCSM (https://biosig.lab.uq.edu.au/pkcsm/), accessed on March 1, 2024. Furthermore, the drug-likeness scores were measured by using the Molsoft LLC website, (https://www.molsoft.com/mprop/ (accessed on March 6, 2024), Importantly, Lipinski's rule of five (ROF) was determined to screen the opportunity of the above medicinal herbals to serve as a standard drug [33, 34].

RESULTS

The binding sites of BTG2 protein

The binding sites elucidated the specific amino acids available for binding to the ligand. The binding sites are divided into two categories: hydrogen bond interaction, including the combination between protein (BTG2) and ligand through a hydrogen bond, and non-hydrogen interaction, involving covalent interaction between ligand and protein. Figure 2a illustrates the highest possibility of interacting with ligands via a covalent bond: HIS 49 has a high non-bond interaction with 11%; the following high non-bond interaction percentages were Ser21 and TRP 103 with percentages of 10.3 and 9.8, respectively. Figure 2b revealed the probability of the specific amino acid combining with the ligand throughout the H-bond interaction. The amino acids that can bind to ligands by hydrogen bond were HIS 49 and ASP 75, with 14 and 10%, respectively. Hence, the amino acid HIS 49 in the BTG2 protein can improve the combination with the ligand.

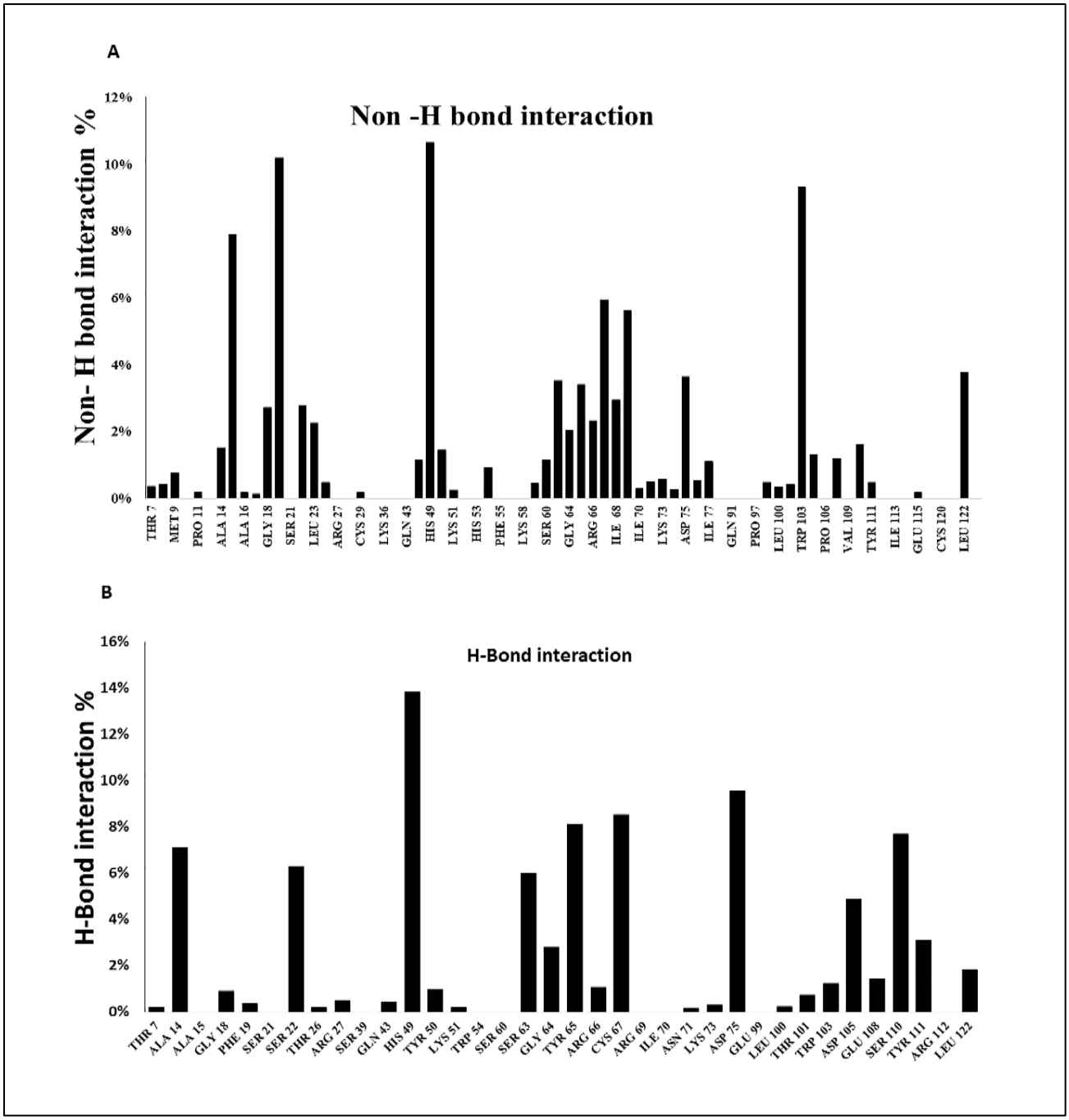

Figure 2: Binding Site Map of the Target Protein (BTG2). A) FT mapping for non-H bond interaction. B) FT mapping for H-interaction

Gene Ontology Analysis

- **PPI interaction**

Figure 3A demonstrated that the number of BTG2-related targets (nodes) was 21, the edges between targets were 101, the average node degree was 9.62, and the PPI enrichment P-value was less than 10 e^{-16}. The main protein that interacts with BTG2 is total protein 53 (TP53). TP53 regulates the transcription of the addition of cell cycle genes such as CCR4-NOT (CNOT6), CNOT6L, CNOT7, CNOT8, CNOT9, CNOT10, and CCNOT11. the CNOT gene family, CCR4-not transcriptional regulation, as well as the deadenylase complex. The CNOT gene was functionalized as a regulator of transcription and DNA templated. Interestingly, BTG2 also interacts with growth arrest and the DNA-damage-inducible protein GADD45 alpha, which contribute to treatment with DNA-damaging agents (mutagens). Also, GADD45A is interceded via the P53 mechanism (independent and dependent mechanisms). Also, it contributes to the activation of the p38/JNK pathway by activating the MTK1/MEKK4 kinase. In addition, BTG2 is related to Fos proto-oncogene (FOS), which enters the apoptosis process. The Fos gene is expressed mainly in bone marrow.

- ***ShinyGO***

Figure 3B displays the KEGG pathway enrichment with fold enrichment scores (FDR) as well as a tree. The enrichment analysis shows the differentially expressed genes were magnificence enriched in RNA degradation, thyroid cancer, colorectal cancer, endometrial cancer, Basel cell carcinoma, melanoma, non-small cell lung cancer, P53 signaling pathway, glioma, pancreatic cancer, chronic myeloid leukemia, apoptosis, small cell lung cancer, breast cancer, NF-β kaβ signaling pathway and MAPK signaling pathway. Figure 3C highlights the relation between BTG2 and RNA degradation with similar score of 4.6 e^{-12}, MAPK signaling pathway has 2.1 e^{-3}, NF kaβ singling pathway has $5e^{-2}$, small cell lung cancer has 4.2 e^{-2}, chronic myeloid leukemia, pancreatic cancer, Basel cell carcinoma, pancreatic cancer, melanoma, non-small cell lung cancer, P53 signaling pathway, endometrial cancer glioma, and has the same value branch $3.1e^{-2}$. Breast cancer, apoptosis, and thyroid cancer have the same value of 1.8 e^{-2}. Finally, colorectal cancer has 6.9 e^{-3}. Figure 3D represents the schematic diagram of the contribution of BTG2 in the P53 signaling pathway in chronic myeloid leukemia throughout GADD45A.

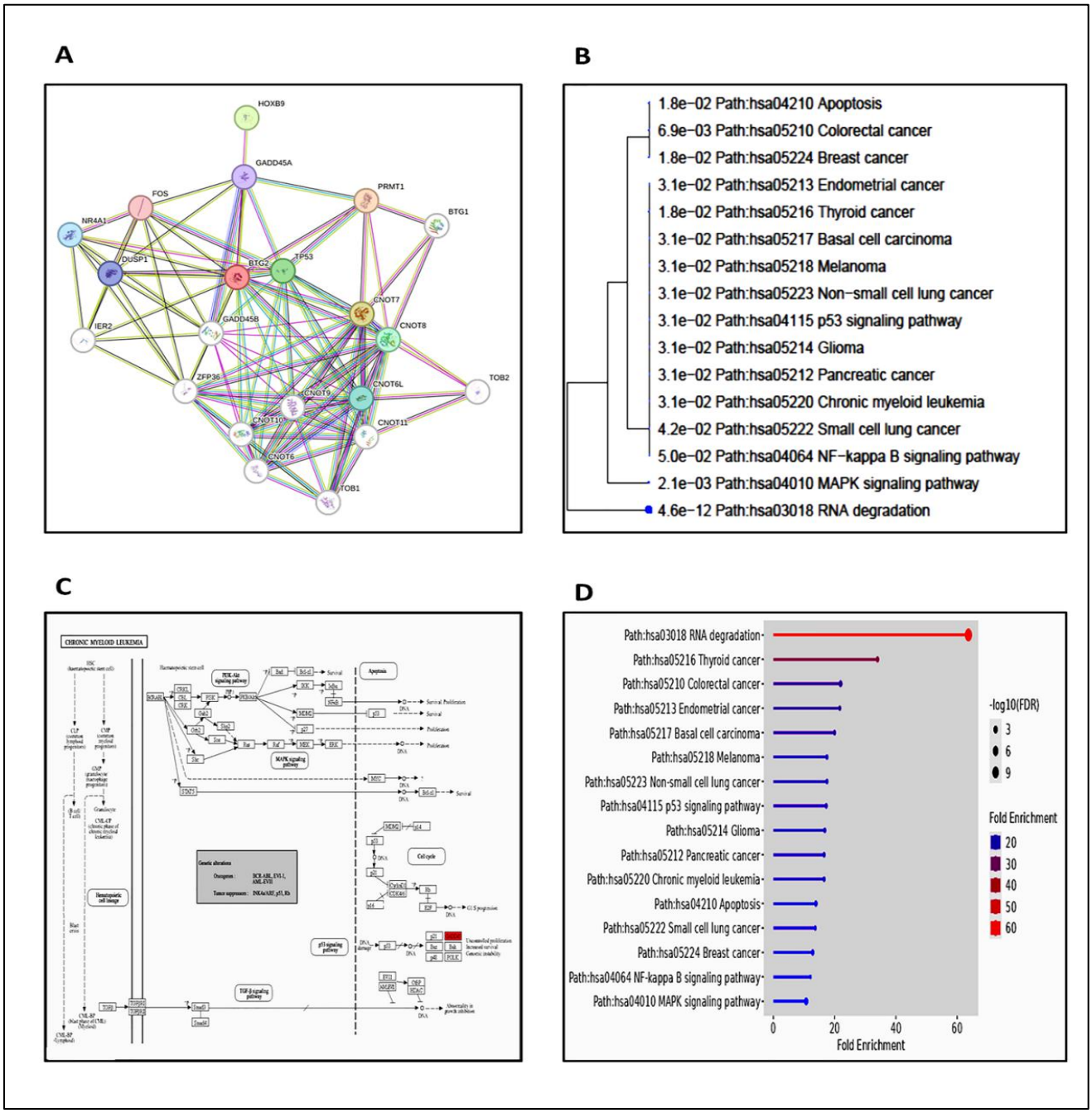

Figure 3: A) PPI of the Target Protein (BTG2). B) Tree of Target BTG2 Protein. C) Biological pathway of BTG2 protein. D) KEGG pathway enrichment of BTG2 protein

- **Wiki pathway**

The Wiki pathway was investigated to determine the importance of BTG2 protein during the biological pathway. The Wiki pathway obtained by applying the Cytoscape website (https://cytoscape.org/). The *BTG2* gene enters the cell cycle process with *GADD45* during the *P53* transcription regulation with a similarity of 0.13 and a P-value equal to 1.37 e^{-2}. It indicated the importance of BTG2 in the P53 regulation process (dependent and independent), as illustrated in figure 4.

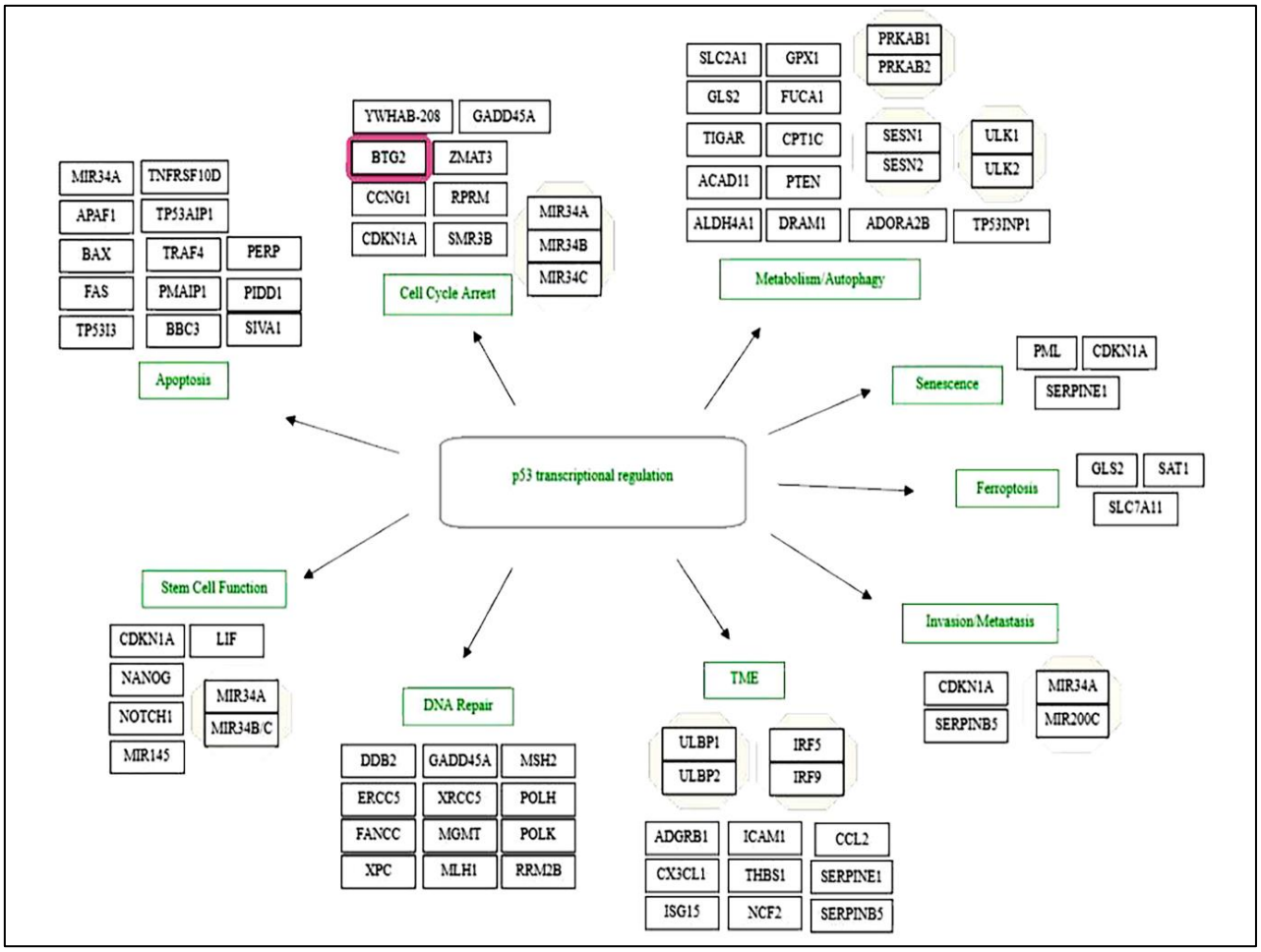

Figure 4: The Wiki pathway of BTG2 contributes to the P53 transcription regulation pathway

Molecular docking

Figures 5 and 6 displayed the interaction between phytochemical medicines and the targeting protein BTG2 (3DJU) throughout the molecular docking simulation. Hesperidin interacts with BTG2 through H-bonds with His 49, Cys 67, Arg 69, Asn 71, Asp 75, Arg 112, and Thr 101, with distance bond lengths of 2.35 A˚, 2.79 A˚, 2.78 A˚, 2.41 A˚, 2.54 A˚, 2.43 A˚ , and 2.76 A˚, respectively. The ΔG of the interaction of hesperidin with BTG2 is equal to -7.0 kcal/mol, as figures 5a, and 5b revealed. In addition, the BTG2 protein binds to hesperidin by carbon-hydrogen via Glu 99 and Pro 76, with bond lengths equal to 3.6 and 3.6, respectively. Ligustroside interacts with BTG2 by h-bond binding with Cys 67, Arg 69, Ile 70, Asn 71, His 72, and Asp 75 with distance bond lengths of 2.02 A˚, 2.21 A˚, 2.5 A˚, 2.31 A˚, 2.3 A˚, and 2.6 A˚, respectively. The ΔG of the interaction of Ligustroside with BTG2 equals 6.1 kcal/mol. As figures 5b, and 6b. Salidroside interacts with BTG2 by h-bond binding with Typ 65, Arg 69, and Asn 71, with distance bond lengths of 1.87 A˚ and 2.98 A˚, respectively. While Arg 69 and Lys 73 interact with BTG2 through the pi-alkyl bond, their bond lengths were 4.25 A˚ and 5.45 A˚, respectively. The ΔG of the interaction of salidroside with BTG2 is equal to -6.1 kcal/mol as figures 5c, and 6c shown. Oleuropein can bind to BTG2 through hydrogen bonds His 49, Asn 71, Lys 73, and Arg 80, with bond lengths of 2.37 A˚, 2.53 A˚, 2.37 A˚, and 2.37 A˚. Also, oleuropein binds to Cys 67 by a carbon-hydrogen bond with a bond length of 3.51A. In addition, oleuropein interacts with Arg 69 by a pi-alkyl bond with a bond length of 4.22 as figures 5d, and 6d displayed. The ΔG of the interaction of oleuropein with BTG2 is equal to -6.1 kcal/mol. Hesperetin can bind to BTG2 through hydrogen bonds with the following amino acids: Arg 69 and Asp 75, with bond lengths equal to 2.3 A˚ and 2.41 A˚. While the other amino acids His 72 and Lys 73 bind to hesperetin by a

pi-alkyl bond with binding energies of 4.20 A˚ and 4.88 A˚, respectively. Additionally, Arg amino acid combines with hesperetin by a p-cation bond with a bond length of 4.15 A˚. The ΔG of the interaction of hesperetin with BTG2 is equal to -5.6 kcal/mol (Figures 5e, and 6e). Gallic acid combines with BTG2 by associating a hydrogen bond by interacting with gallic acid and the following amino acids: Arg 69, Iil 70, Glu 99, and Thr 101, with bond lengths equal to 2.84 A˚, 1.83 A˚, 2.42 A˚, and 2.57 A˚. Gallic acid forms a carbon-hydrogen bond with Glu 115 with a bond length of 3.71. The ΔG of the interaction of gallic acid with BTG2 is equal to -4.7 kcal/mol (Figures 5f, and 6f). Cinnamic acid interacts with BTG2 by h-bond binding with His 49 and Cys 67, with bond lengths of 2.25 A˚ and 2.16 A˚, respectively. While Arg 69, and Lys 73 amino acids bind to cinnamic acid by a pi-alkyl bond with bond lengths of 4.16 A˚ and 5.31 A˚, respectively, the ΔG of the interaction of cinnamic acid with BTG2 is equal to -4.6 kcal/mol (Figures 5g, and 6g). Cytarabinee and daunorubicin are standard drugs used to treat AML patients. Cytarabinee interacts with BTG2 by h-bond binding with His 49, Asn 71, and Asp 75, with bond lengths of 2.91 A˚, 2.42 A˚, and 2.37 A˚, respectively. While Arg 69 amino acid binds to Cytarabine by pi-alkyl bond with energy 5.04, the ΔG of the interaction of Cytarabinee with BTG2 is equal to -5.0 kcal/mol (Figures 5h, and 6h). Daunorubicin interacts with BTG2 by h-bond binding with Typ 65 and Lys 73, with bond lengths of 2.37 A˚ and 2.40 A˚, respectively. Arg 69 combines with daunorubicin by a carbon-hydrogen bond with a bond length of 2.45 A˚. Pro 76 amino acid interacts with Daunorubicin by pi-alkyl with a bond length of 5.03 A˚. The ΔG of the interaction of daunorubicin with BTG2 is equal to -5.8 kcal/mol, as figures 5i, and 6i displayed.

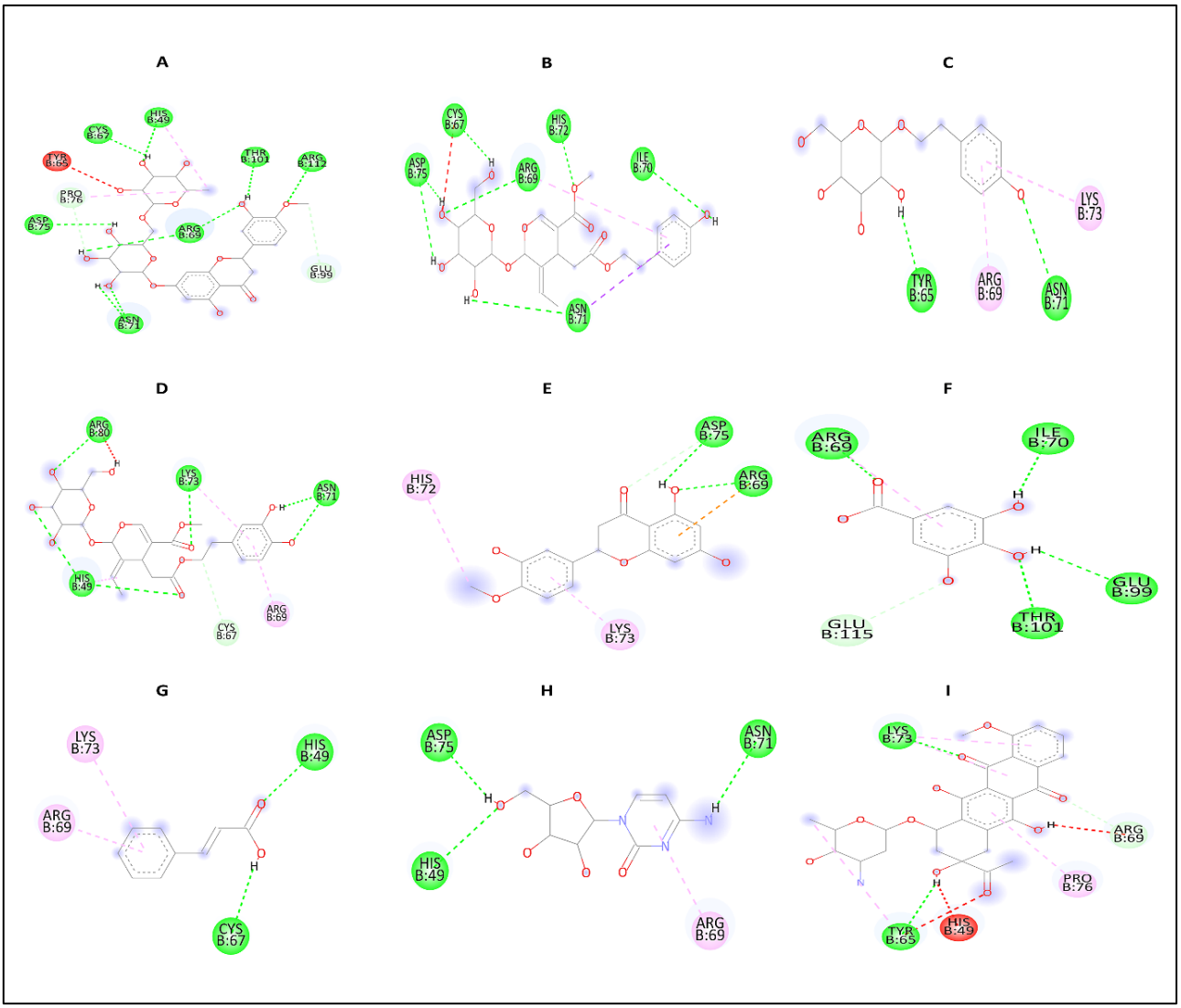

Figure 5: The molecular docking of BTG2 with docked phytochemical herbs as 2D representation. A) Hesperidin. B) Ligustroside. C) Salidroside. D) Oleuropein. E) Hesperetin. F) Gallic acid. G) Cinnamic acid. H) Cytarabine and I) Daunorubicin

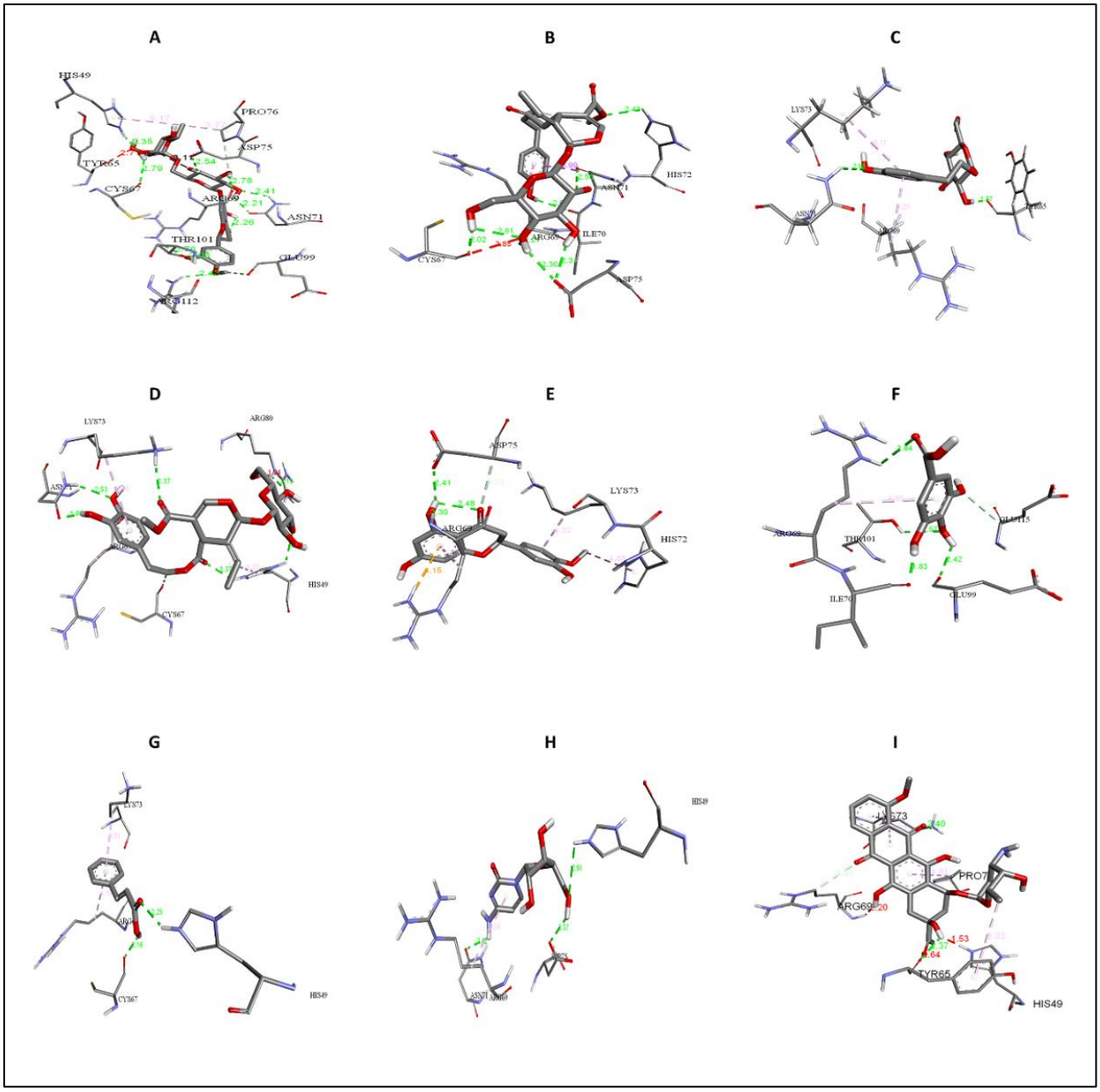

Figure 6: The molecular docking of BTG2 with docked phytochemical herbs as 3D representation. A) Hesperidin. B) Ligustroside. C) Salidroside. D) Oleuropein. E) Hesperetin. F) Gallic acid. G) Cinnamic acid. H) Cytarabine. and I) Daunorubicin

Molecular Dynamic simulation

The purpose of this work is to study the conformational change in BTG2 protein when it interacts with the leading compound, hesperidin, compared with the unbound protein state (Apo) of BTG2. This investigation was determined via molecular dynamics (MD) simulations lasting 100 nanoseconds (ns), Key structural parameters, including root-mean-square deviation (RMSD), radius of gyration (Rg), and solvent accessible surface area (SASA), which were calculated using the GROMACS software package, with the complex re-centered and re-wrapped within the unit cells before analysis.

Figure 7A displays the fluctuations around 1.40 nm for the apoprotein, suggesting inherent flexibility, while the slight decrease in Rg to 1.37 nm upon binding with limonin indicates a more compact or stabilized conformation of the protein-Hesperidin complex. The alternation of Rg is indirectly dependent on the flexibility of the protein structure.

Figure 7B illustrates the root mean square deviation (RMSD) of the protein without hydrogens, reflecting the degree of deviation in protein conformations throughout the simulation. The fluctuations of all complexes, including BTG2 (Apo) protein, were observed towards the end of the simulation, indicating a magnificent change in protein

conformations. The interaction with Hesperidin induced higher RMSD fluctuation, increasing from 0.5 to 1.5 nm at 20 ns by the simulation's conclusion. Furthermore, the compactness of the protein backbone across the three complexes was assessed through Rg analysis during the simulation period. Interaction with Hesperidin induced higher RMSD fluctuation, increasing from 0.2 to 0.4 nm at 20 ns by the simulation's conclusion. Furthermore, the compactness of the protein backbone across the complexes was assessed through Rg analysis during the simulation period, as shown in Figure 7B.

BTG2 demonstrated enhanced compactness and stability in its Apo state. But when APO protein interacted with the Hesperidin complex, it remained stable until around 20 ns before experiencing a sharp increase in fluctuation, with the RMSD jumping from 0.2 to 20 nm. These findings highlight the dynamic nature of protein conformations and underscore the influence of ligand binding on protein stability and structural dynamics throughout the simulation period.

In Figure 7C, the root mean square fluctuation (RMSF) analysis reveals the variability in atomic positions within the protein structure across different regions. All two complexes display similar RMSF patterns, with residues involved in ligand interactions exhibiting minimal fluctuation (<0.2 nm). The first and last 50 residues show slight changes, indicating flexibility and distance from the binding pocket.

In Figure 7D, the solvent-accessible surface area (SASA) analysis reveals differences in the exposed surface area of the protein-ligand complexes. particularly the SASA area for the protein-hesperidin complex, which consistently remained the lowest, fluctuating between 70 and 66 nm. The binding stability was studied by determining the number of H-bonds formed during simulation time (100 ns). Hesperidin forms four stable H-bonds, as shown in Figure 7E. The behavior aligns with the RMSD plot. Figure 7F illustrates the large number of hydrophobic residues, including a great amount of energy in Hesperidin binding to its active pocket with a high energy range of -3 to -6 Kcal/mol. The key interactions in the BTG2-Hesperidin complex appear to be Arg 69.

ADMET and Drug-Likeness Properties

The aim is to study the ADMET properties of the phytochemicals to certify the accessibility of the following herbal medicine as a feasible and desirable drug. Tables 1 and 2 summarize the parameters depending on Lipinski's rules to determine the best herbal that can be recommended as a drug. The molecular weights of the following phytochemicals: Hesperidin, Ligustroside, Salidroside, Oleuropein, Hesperetin, Gallic acid, and Cinnamic acid are 610.565, 524.519, 300.307, 540.518, 302.282, 170.12, and 148.161, respectively. The number of hydrogen bond acceptors is the following: 15, 12, 7, 13, 6, 4, and 1 for Hesperidin, Ligustroside, Salidroside, Oleuropein, Hesperetin, Gallic Acid, and Cinnamic Acid, respectively. The number of hydrogen bond donors is the following: 8, 5, 5, 6, 3, 4, and 1 for Hesperidin, Ligustroside, Salidroside, Oleuropein, Hesperetin, Gallic Acid, and Cinnamic Acid, respectively. The synthetic accessibility of Hesperidin, Ligustroside, Salidroside, Oleuropein, Hesperetin, Gallic Acid, and Cinnamic Acid is 6.34, 6.18, 4.26, 6.22, 3.22, 1.22, 1.67, 3.84, and 5.77, which indicates that Hesperidin, Ligustroside, Salidroside, and Oleuropein can be synthesized, while Hesperetin, Gallic Acid, and Cinnamic Acid can be prepared easier or harder in the laboratory or manufacturing according to the scale of synthesis, which ranges from 1 (easy to prepare) to 10 (hard to prepare).

The bioavailability of Hesperidin, Ligustroside, Salidroside, Oleuropein, Hesperetin, Gallic acid, and Cinnamic acid was 0.17, 0.11, 0.55, 0.11, 0.55, 0.56, and 0.85. Cytochrome P450 protein families responsible for the metabolism of drugs include 1A2, 2C9, 2C19, 2D6, and 3A4, among which the most important is the 3A4 enzyme. All the phytochemical herbs are non-toxic. Figure 8 refers to the possibility of the compounds being an efficient drug. Hesperidin, oleuropein, hesperetin, Cytarabine, and daunorubicin have a positive value, which indicates the tendency of the above compounds to use drugs. Finally, hesperidin showed accessibility and ADMET properties; hence, it can be assessed as a potential drug agent.

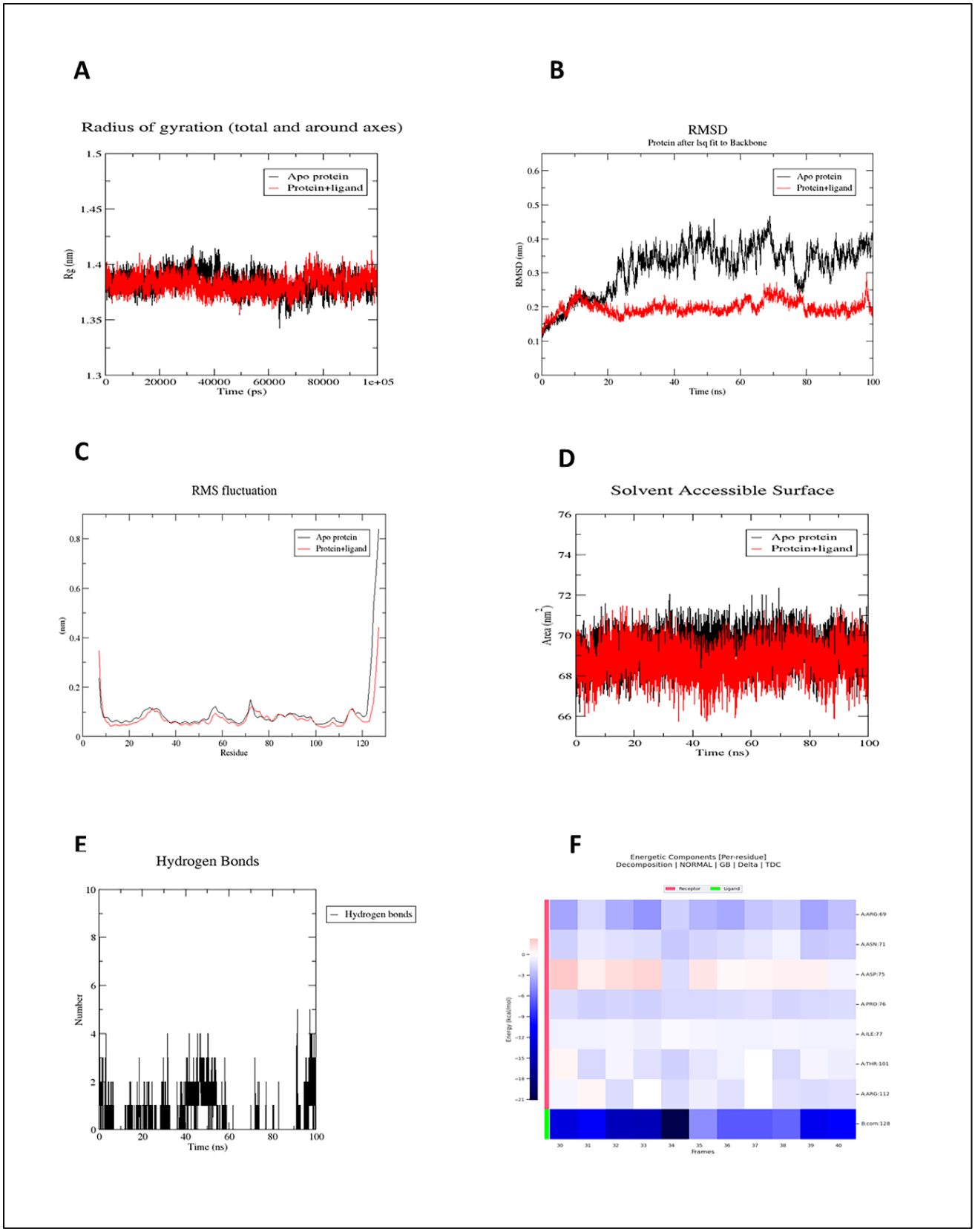

Figure 7: Molecular dynamics simution of the BTG2 inteacts with Hesperidin. A) RMSD of Structural dynamics of BTG2. B) Radius of gyration of Structural dynamics of BTG2. C) RMS fluctation of gyration of BTG2 during Molecular dynamics simution. D) Complexes SASA values of BTG2 during Molecular dynamics simution. E) Number of H- Bond between BTG2 target with the Hesperidin. F) Residues energetic components binding free energies estimated for BTG2 target with the Hesperidin hits by MM/GBSA method.

Table 1: Drug-likeness properties of Phytochemical compounds and standard leukemia drugs

Compound	Absorption Intestinal Human Absorption	Distribution		Metabolism								AMES Toxicity
		Log p	Log S	CYP2D6 Substrate	CYP3A4 Substrate	CYP1A2 Inhibitior	CYP2C19 Inhibitior	CYP2C9 Inhibitior	CYP2D6 Inhibitior	CYP3A4 Inhibitior	Total Clearance	
Hesperidin	31.481	-1.1566	-4.33	No	No	No	No	No	No	No	0.211	No
Ligustroside	52.557	-0.3398	-0.3398	No	No	No	No	No	No	No	1.428	No
Salidroside	45.49	-1.2488	-0.97	No	No	No	No	No	No	No	0.187	No
Oleuropein	44.206	-0.6342	-2.38	No	No	No	No	No	No	No	1.176	No
Hesperetin	70.277	2.5185	-4.27	No	Yes	No	No	No	No	No	0.044	No
Gallic Acid	43.374	0.5016	-2.34	No	No	No	No	No	No	No	0.518	No
Cinnamic Acid	94.833	1.7844	-2.54	No	No	Yes	No	Yes	No	No	0.781	No
Cytarabinee	58.476	-2.563	-0.09	No	No	No	No	No	No	No	0.503	No
Daunorubicin	73.176	1.0289	-5.35	No	No	No	No	No	No	No	1.026	No

Table 2: Drug-likeness properties of Phytochemical compounds and standard leukemia drugs

Compound	Molecular Weight	HBA	HBD	mlogP	Synthetic Accessibility	Bioavailability	Lipinski Violation	Drug Likeness
Hesperidin	610.565	15	8	-3.04	6.34	0.17	3	No
Ligustroside	524.519	12	5	-0.86	6.18	0.11	2	No
Salidroside	300.307	7	5	-1.22	4.26	0.55	0	yes
Oleuropein	540.518	13	6	-1.34	6.22	0.11	3	No
Hesperetin	302.282	6	3	0.41	3.22	0.55	0	Yes
Gallic Acid	170.12	4	4	-0.16	1.22	0.56	0	Yes
Cinnamic Acid	148.161	1	1	1.90	1.67	0.85	0	Yes
Cytarabinee	243.219	8	4	-2.29	3.84	0.55	0	Yes
Daunorubicin	527.526	11	5	-1.35	5.77	0.17	2	No

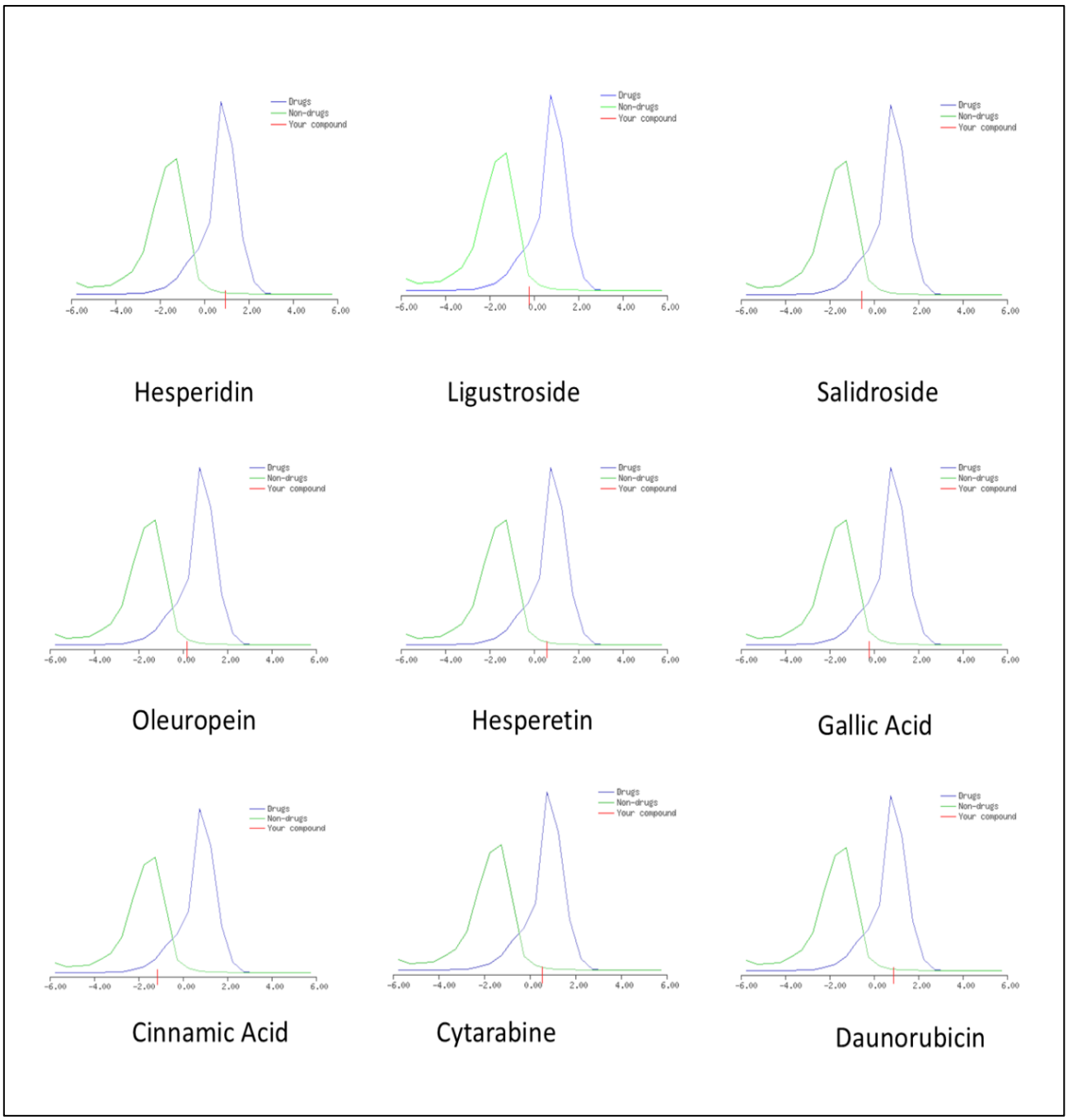

Figure 8: Drug-Likeness scores of the Phytochemicals compounds

DISCUSSION

Acute myeloid leukemia is defined as the uncontrolled growth of abnormal leucocytes inside bone marrow and peripheral blood cells. one-third of AML patients are young. The main issue is the resistance of AML to conventional therapy like Cytarabinee, anthracycline, and daunorubicin [35, 36]. BTG2 belongs to the BTG/TOB gene family. It contributes to many biological pathways, such as cell cycle regulation, DNA damage repair, and cell proliferation and differentiation [37]. Both BTG1 and BTG2 are tumor suppressors against lymphoma and solid tumors. Interestingly, BTG1 and BTG2 are capable of protecting cells from any neoplastic transformation. Furthermore, it has the essential function of controlling and regulating gene expression through interaction with transcriptional cofactors [38]. In this study, the PPI interaction illustrated the relationship between BTG2 and RNA degradation. Many studies have exhibited the activity of BTG1/BTG2 deadenylation and degradation of mRNA [39]. Importantly, the PPI analysis exhibited a relationship between BTG2 and many cancer types. Previous articles demonstrated the relationship between the expression level of BTG2 and many cancer types, such as bladder cancer [40], pancreatic cancer [41], and lung cancer [42]. BTG2 enters the P-53 pathway through cell cycle arrest, as shown in Figure 4 [43]. BTG2 has a crucial role in cell growth. Past studies showed the

activity of cisplatin to ameliorate protestant cancer cell proliferation by decreasing the expression level of BTG2 via the p53-dependent pathway or the p53-independent NF-κB pathway [44]. Ryu et al reported that BTG2 is increased by PKC-δ in U937 cells, and induces G2/M arrest and cell death through restricted cyclin B1-Cdc2 binding [45]. BTG2 stimulates PRMT1 (protein arginine methyltransferase 1), also, it induces and accelerates the promotion of DNA repair in DSBs and Mre 11 methylation [46-47]. Interearingly. BTG2 induces apoptosis by upregulating the Bax gene [48]. Hence, BTG2 has a vital role in tumor progression and development. Currently, scientists focus on the utilization of natural products, particularly to attenuate and inhibit the activity of cancer cell proliferation and progressive pathways. In this study, the phytomedicine herbals were used to study its activity against BTG2 which has good activity as an anti-cancer agent, comparable with standard drugs against AML like Cytarabinee and daunorubicin. Interestingly, the application of computerization insights studies, including molecular docking and molecular dynamics simulation, as well as studying the toxicity and biocompatibility of the selective compound, has had a great effect on the advancement and development of the pharmaceutical industry and saved a crucial amount of time to improve and fabricate novel drugs against difficult diseases such as cancer. In our work, molecular docking, molecular dynamics simulations, and pharmacokinetics were used to assess the ability of Hesperidin, Ligustroside, Salidroside, Oleuropein, Hesperetin, Gallic acid, Cinnamic acid, Cytarabinee, and daunorubicin to inhibit BTG2. Hesperidin has the highest binding scoring due to the interaction of hesperidin with BTG2 amino acid residues such as His 49, Cys 67, Arg 69, Asn 71, Asp 75, Arg 112, and Thr 101 by H-bond interaction (Fig 5a, Fig 6a). The ΔG equals -7 kcal/mol, while the standard drugs (Cytarabinee, and daunorubicin) have a ΔG equal to -5, and 5.8 kcal/mol for Cytarabinee daunorubicin, respectively. Previous studies demonstrated a significant impact of Hesperidin on the prevention of cancer by restricting the cell cycle in MG-63 cell lines of human osteosarcoma. Hesperidin interacts with the G2/M phase of cell cycle arrest at high doses [48, 49]. Furthermore, another study exhibited the downregulation of STAT3, STAT2, and STAT1 activity in endometrial carcinoma cells as a result of Hesperidin administration at high doses [50]. Interestingly, Hesperidin-stopping hepatocarcinogenesis occurred with diethylnitrosamine (DEN) through suppressing the PI3K/Akt signaling pathway. Another work illustrated that Hesperidin stimulates ERK1/2 and leads to paraptosis [51]. The molecular dynamics simulation has studied the validity of the BTG2-hesperidin interaction. The MD study aims to exhibit the dynamic behavior of BTG2 and Hesperidin. Also, the determination of the residue of the active site in BTG2 is needed to work out the catalytic interaction with the ligand (Hesperidin) and evaluate the number of H-bonds that will be performed during the simulation time (100 ns) [46]. In our study, figure 7B reveals the fluctuations of all complexes containing BTG2 protein that were observed towards the end of the simulation, which indicated a significant change in protein conformations. According to Schreiner and colleagues, the RMSD refers to the degree of deviation in protein and protein-ligand complexes due to changes in protein conformation. Hence, the stability of the predicted docking BTG2-hesperidin complex (Figure 7b, 7c) provides a significant change in protein conformation. Interestingly, figure 7f exhibits the highest number of catalytic residues in all proteins that can interact with ligands; the Agr 69 residue in the BTG2 protein has a high energy range of -3 to -6 kcal/mol. This result agrees with the FT mapping in figures 1a, and 1b, which indicates the best catalytic positive or residue to interact with ligand, as well as the docking of BTG2 with Hesperidin; hence, the MD confirmed the predicted docking between BTG2 and Hesperidin. The pharmacokinetics of the phytomedicinal herb mentioned above illustrated the advantages of using Hesperidin as a potential drug against BTG2 for many reasons, like non-toxicity, bioavailability, and synthetic accessibility. Finally, Hesperidin has been made into a stability complex with BTG2 by applying molecular docking and molecular dynamics simulation, also, the pharmacokinetics and Lipinski's rule.

CONCLUSION

In this study, protein-protein interactions, gene ontology, and gene enrichment analysis were investigated to identify the biological pathways related to BTG2 gene. Then, we examined the pharmacokinetic properties and toxicity of a group of flavonoid medicinal herb compounds and drugs using the SwissADME, pkCSM, and Molsoft LLC websites. Interestingly, the molecular docking between the medicinal herbs and AML-standard drugs against the human BTG2 protein was performed by Auto-dock Vina, and molecular dynamics simulation was executed by the GROMACS software package to study the behavior between the BTG2 protein and the protein-ligand complex. The results highlighted that the PPI interrelates with those found in P53 transcriptional gene network pathways, and gene enrichment analysis exhibited that RNA degradation was the most significant enrichment pathway. The results showed that Hesperidin displayed the highest docking score of −7.0 kcal/mol when interacting and docking against the BTG2 protein, while Cytarabinee and Daunorubicin had docking scores of 5.0 and 5.8, respectively. The molecular dynamics results show conformational alterations with surface residue fluctuation in BTG2 protein. The best residue in the BTG2 protein is Arg 69. Finally, hesperidin is a potential drug against leukemia by inhibiting BTG2 in computation insight, but we recommend performing more in vitro and in vivo studies.

Data Availability Statement

The original contributions presented in the study are included in the article Material; further inquiries can be directed to the corresponding author.

Conflicts of Interest: The authors declare no conflicts of interest.

Author Contributions

Conceptualization: A.H, S.E.H., and E.A.E.; formal analysis: A.H S.E.H., and E.A.E.; funding acquisition: A.H, S.E.H., and E.A.E.; investigation: A.H, S.E.H., and E.A.E.; A.H, S.E.H., and E.A.E.; project administration: A.H, S.E.H., and E.A.E and resources: A.H, S.E.H., and E.A.E.; supervision: A.H, S.E.H., and E.A.E.; validation A.H, S.E.H., and E.A.E.; visualization: A.H, S.E.H., and E.A.E.; writing—original draft: A.H.; writing—review edition: A.H, S.E.H., and E.A.E. All authors have read and agreed to the published version of the manuscript.

ACKNOWLEDGMENTS

The corresponding author would like to thank the Genetic Engineering and Biotechnology Research Institute (GEBRI), University of Sadat City, and the School of Biotechnology, Nile University.

List of Abbreviations

- CNOT6: CCR4-NOT transcription complex subunit 6
- CNOT7: CCR4-NOT transcription complex subunit 7
- CNOT8: CCR4-NOT transcription complex subunit 8
- CNOT9: CCR4-NOT transcription complex subunit 9
- CNOT10: CCR4-NOT transcription complex subunit 10
- CNOT 11: CCR4-NOT transcription complex subunit 11

REFERENCES

1. Li, Z., Chen, B., Wang, P., Li, X., Cai, G., Wei, W., & Dong, W. (2016). A proteomic analysis of acute leukemia cells treated with 9-hydroxyoctadecadienoic acid. *Lipids in Health and Disease*, 15, 1-8. https://doi.org/10.1186/s12944-016-0359-4
2. Lindsley, R. C., Mar, B. G., Mazzola, E., Grauman, P. V., Shareef, S., Allen, S. L., ... & Ebert, B. L. (2015). Acute myeloid leukemia ontogeny is defined by distinct somatic mutations. *Blood, The Journal of the American Society of Hematology*, *125*(9), 1367-1376. https://doi.org/10.1182/blood-2014-11-610543
3. Lai, Y., OuYang, G., Sheng, L., Zhang, Y., Lai, B., & Zhou, M. (2021). Novel prognostic genes and subclasses of acute myeloid leukemia revealed by survival analysis of gene expression data. *BMC Medical Genomics*, *14*(1), 1-10. https://doi.org/10.1186/s12920-021-00888-0
4. Yang, W., Wei, C., Cheng, J., Ding, R., Li, Y., Wang, Y., ... & Wang, J. (2023). BTG2 and SerpinB5, a novel gene pair to evaluate the prognosis of lung adenocarcinoma. *Frontiers in Immunology*, *14*, 1098700. https://doi.org/10.3389/fimmu.2023.1098700
5. Liu, S., Xu, H., & Li, Z. (2023). Linoleic acid derivatives target miR-361-3p/BTG2 to confer anticancer effects in acute myeloid leukemia. *Journal of Biochemical and Molecular Toxicology*, *37*(11), e23481. https://doi.org/10.1002/jbt.23481
6. Mao, B., Zhang, Z., & Wang, G. (2015). BTG2: a rising star of tumor suppressors. *International journal of oncology*, *46*(2), 459-464. https://doi.org/10.3892/ijo.2014.2765
7. Taneja, S. C., & Qazi, G. N. (2007). Bioactive Molecues in Medicinal Plants: A perspective in their therapeutic action. *Drug discovery and development*, 1, 1-50. https://doi.org/10.1002/9780470085226.ch17
8. Desai, A. G., Qazi, G. N., Ganju, R. K., El-Tamer, M., Singh, J., Saxena, A. K., ... & Bhat, H. K. (2008). Medicinal plants and cancer chemoprevention. *Current drug metabolism*, *9*(7), 581-591. https://doi.org/10.2174/138920008785821657
9. Rahmani, A. H., Babiker, A. Y., & Anwar, S. (2023). Hesperidin, a bioflavonoid in cancer therapy: a review for a mechanism of action through the modulation of cell signaling pathways. *Molecules*, *28*(13), 5152. https://doi.org/10.3390/ molecules28135152
10. Emma, M. R., Augello, G., Di Stefano, V., Azzolina, A., Giannitrapani, L., Montalto, G., ... & Cusimano, A. (2021). Potential uses of olive oil secoiridoids for the prevention and treatment of cancer: a narrative review of preclinical studies. *International journal of molecular sciences*, *22*(3), 1234. https://doi.org/10.3390/ijms22031234
11. Torić, J., Karković Marković, A., Jakobušić Brala, C., & Barbarić, M. (2019). Anticancer effects of olive oil polyphenols and their combinations with anticancer drugs. *Acta Pharmaceutica*, *69*(4), 461-482. https://doi.org/10.2478/acph-2019-0052
12. Ruzzolini, J., Peppicelli, S., Bianchini, F., Andreucci, E., Urciuoli, S., Romani, A., ... & Calorini, L. (2020). Cancer glycolytic dependence as a new target of olive leaf extract. *Cancers*, *12*(2), 317. https://doi.org/10.3390/cancers12020317
13. Ge, C., Zhang, J., & Feng, F. (2019). Salidroside enhances the anti-cancerous effect of imatinib on human acute monocytic leukemia via the induction of autophagy-related apoptosis through AMPK activation. *RSC advances*, *9*(43), 25022-25033. DOI: 10.1039/C9RA01683J
14. Zhuang, X., Maimaitijiang, A., Li, Y., Shi, H., & Jiang, X. (2017). Salidroside inhibits high-glucose induced proliferation of vascular smooth muscle cells via inhibiting mitochondrial fission and oxidative stress. *Experimental and Therapeutic*

Medicine, *14*(1), 515-524. https://doi.org/10.3892/etm.2017.4541
15. Ju, L., Wen, X., Wang, C., Wei, Y., Peng, Y., Ding, Y., ... & Shu, L. (2017). Salidroside, a natural antioxidant, improves β-cell survival and function via activating AMPK pathway. *Frontiers in Pharmacology*, *8*, 749. https://doi.org/10.3389/fphar.2017.00749
16. Gu, R., Zhang, M., Meng, H., Xu, D., & Xie, Y. (2018). Gallic acid targets acute myeloid leukemia via Akt/mTOR-dependent mitochondrial respiration inhibition. *Biomedicine & Pharmacotherapy*, 105, 491-497. https://doi.org/10.1016/j.biopha.2018.05.158
17. Reddy, T. C., Reddy, D. B., Aparna, A., Arunasree, K. M., Gupta, G., Achari, C., ... & Reddanna, P. (2012). Anti-leukemic effects of gallic acid on human leukemia K562 cells: Downregulation of COX-2, inhibition of BCR/ABL kinase and NF-κB inactivation. *Toxicology in Vitro*, *26*(3), 396-405. https://doi.org/10.1016/j.tiv.2011.12.018
18. Wang, R., Ma, L., Weng, D., Yao, J., Liu, X., & Jin, F. (2016). Gallic acid induces apoptosis and enhances the anticancer effects of cisplatin in human small cell lung cancer H446 cell line via the ROS-dependent mitochondrial apoptotic pathway. *Oncology reports*, *35*(5), 3075-3083. https://doi.org/10.3892/or.2016.4690.
19. De, P., Baltas, M., & Bedos-Belval, F. (2011). Cinnamic acid derivatives as anticancer agents-a review. *Current medicinal chemistry*, *18*(11), 1672-1703.
20. Yang, X., Morita, M., Wang, H., Suzuki, T., Yang, W., Luo, Y., ... & Rao, Z. (2008). Crystal structures of human BTG2 and mouse TIS21 involved in suppression of CAF1 deadenylase activity. *Nucleic acids research*, *36*(21), 6872-6881.
21. Kozakov, D., Grove, L. E., Hall, D. R., Bohnuud, T., Mottarella, S. E., Luo, L., ... & Vajda, S. (2015). The FTMap family of web servers for determining and characterizing ligand-binding hot spots of proteins. *Nature protocols*, *10*(5), 733-755.
22. Ge, S. X., Jung, D., & ShinyGO, R. Y. A graphical gene-set enrichment tool for animals and plants. *Bioinformatics*, *36*(8), 2628-2629.
23. Kotlyarov, S. (2022). Analysis of differentially expressed genes and signaling pathways involved in atherosclerosis and chronic obstructive pulmonary disease. *Biomolecular Concepts*, *13*(1), 34-54.
24. Otasek, D., Morris, J. H., Bouças, J., Pico, A. R., & Demchak, B. (2019). Cytoscape automation: empowering workflow-based network analysis. *Genome biology*, 20, 1-15.
25. Bader, G. D., & Hogue, C. W. (2003). An automated method for finding molecular complexes in large protein interaction networks. *BMC bioinformatics*, *4*(2), 1-27. https://doi.org/10.1186/1471-2105-4-2
26. Bader, G. D., & Hogue, C. W. (2003). An automated method for finding molecular complexes in large protein interaction networks. *BMC bioinformatics*, *4*(2), 1-27. https://doi.org/10.1186/1471-2105-4-2
27. Rasool, M., Malik, A., Waquar, S., Tul-Ain, Q., Jafar, T. H., Rasool, R., ... & Pushparaj, P. N. (2018). In-silico characterization and in-vivo validation of Albiziasaponin-A, Iso-Orientin, and Salvadorin using a rat model of alzheimer's disease. Frontiers in Pharmacology, 9, 730. https://doi:10.1021/acsomega.3c07239
28. Hanwell, M. D., Curtis, D. E., Lonie, D. C., Vandermeersch, T., Zurek, E., & Hutchison, G. R. (2012). Avogadro: an advanced semantic chemical editor, visualization, and analysis platform. Journal of cheminformatics, 4, 1-17. https://doi10.3390/biomedicines12020279
29. Merecz-Sadowska, A., Isca, V. M., Sitarek, P., Kowalczyk, T., Małecka, M., Zajdel, K., ... & Zajdel, R. (2024). Exploring the Anticancer Potential of Semisynthetic Derivatives of 7α-Acetoxy-6β-hydroxyroyleanone from Plectranthus sp.: An In Silico Approach. *International Journal of Molecular Sciences*, *25*(8), 4529. https://doi:10.3390/ijms25084529
30. Isca, V. M., Sitarek, P., Merecz-Sadowska, A., Małecka, M., Owczarek, M., Wieczfińska, J., ... & Kowalczyk, T. (2024). Anticancer effects of abietane diterpene 7α-Acetoxy-6β-hydroxyroyleanone from plectranthus grandidentatus and its semi-synthetic analogs: an in silico computational approach. *Molecules*, *29*(8), 1807. https://doi:10.3390/molecules29081807
31. Vieira, I. H. P., Botelho, E. B., de Souza Gomes, T. J., Kist, R., Caceres, R. A., & Zanchi, F. B. (2023). Visual dynamics: a web application for molecular dynamics simulation using GROMACS. *BMC bioinformatics*, *24*(1), 107.
32. Hoelm, M., Chowdhury, N., Biswas, S., Bagchi, A., & Małecka, M. (2024). Theoretical Investigations on Free Energy of Binding Cilostazol with Different Cyclodextrins as Complex for Selective PDE3 Inhibition. *Molecules*, *29*(16), 3824. https://doi.org/10.3390/molecules29163824
33. Pires, D. E., Blundell, T. L., & Ascher, D. B. (2015). pkCSM: predicting small-molecule pharmacokinetic and toxicity properties using graph-based signatures. *Journal of medicinal chemistry*, *58*(9), 4066-4072.
34. Daina, A., Michielin, O., & Zoete, V. (2017). SwissADME: a free web tool to evaluate pharmacokinetics, drug-likeness and medicinal chemistry friendliness of small molecules. *Scientific reports*, *7*(1), 42717.
35. Vandewalle, V., Essaghir, A., Bollaert, E., Lenglez, S., Graux, C., Schoemans, H., ... & Havelange, V. (2021). miR-15a-5p and miR-21-5p contribute to chemoresistance in cytogenetically normal acute myeloid leukaemia by targeting PDCD4, ARL2 and BTG2. *Journal of cellular and molecular medicine*, *25*(1), 575-585.

36. Döhner, H., Estey, E., Grimwade, D., Amadori, S., Appelbaum, F. R., Büchner, T., ... & Bloomfield, C. D. (2017). Diagnosis and management of AML in adults: 2017 ELN recommendations from an international expert panel. *Blood, The Journal of the American Society of Hematology*, *129*(4), 424-447.
37. Yuniati, L., Scheijen, B., van der Meer, L. T., & van Leeuwen, F. N. (2019). Tumor suppressors BTG1 and BTG2: Beyond growth control. *Journal of cellular physiology*, *234*(5), 5379-5389.
38. Kim, S. H., Jung, I. R., & Hwang, S. S. (2022). Emerging role of antiproliferative protein BTG1 and BTG2. *BMB reports*, *55*(8), 380.
39. Wagener, N., Bulkescher, J., Macher-Goeppinger, S., Karapanagiotou Schenkel, I., Hatiboglu, G., Abdel-Rahim, M., Abol-Enein, H., Ghoneim, M. A., Bastian, P. J., Muller, S. C., Haferkamp, A., Hohenfellner, M., Hoppe-Seyler, F., & Hoppe Seyler, K. (2013). Endogenous BTG2 expression stimulates migration of bladder cancer cells and correlates with poor clinical prognosis for bladder cancer patients. *Br J Cancer*, 108, 973-982.
40. Mao, B., Zhang, Z., & Wang, G. (2015). BTG2: a rising star of tumor suppressors. *International journal of oncology*, *46*(2), 459-464.
41. Yang, W., Wei, C., Cheng, J., Ding, R., Li, Y., Wang, Y., Yang, Y., & Wang, J. (2023). BTG2 and SerpinB5, a novel gene pair to evaluate the prognosis of lung adenocarcinoma. *Front Immunol*, 14, 1098700. doi: 10.3389/fimmu.2023.109870
42. Chiang, K. C., Tsui, K. H., Chung, L. C., Yeh, C. N., Feng, T. H., Chen, W. T., Chang P. L., Chiang, H. Y., & Juang, H. H. (2014). Cisplatin modulates B-cell translocation gene 2 to attenuate cell proliferation of prostate carcinoma cells in both p53-dependent and p53-independent pathways. *Sci Rep*, 4, 5511.
43. Zhang, Y. J., Wei, L., Liu, M., Li, J., Zheng, Y. Q., Gao, Y., & Li, X. R. (2013). BTG2 inhibits the proliferation, invasion, and apoptosis of MDA-MB-231 triple-negative breast cancer cells. *Tumour Biol*, 34, 1605-1613.
44. Miyata, S., Mori, Y., & Tohyama, M. (2008). PRMT1 and Btg2 regulates neurite outgrowth of Neuro2a cells. *Neurosci Lett*, 445, 162-165.
45. Ryu, M. S., Lee, M. S., Hong, J. W., Hahn, T. R., Moon, E., & Lim, I. K. (2004). TIS21/BTG2/PC3 is expressed through PKC-δ pathway and inhibits binding of cyclin B1-Cdc2 and its activity, independent of p53 expression. *Experimental cell research*, *299*(1), 159-170.
46. Del Puerto, H. L., Martins, A. S., Moro, L., Milsted, A., Alves, F., Braz, G. F., & Vasconcelos, A. C. (2010). Caspase-3/-8/-9, Bax and Bcl-2 expression in the cerebellum, lymph nodes and leukocytes of dogs aturally infected with canine distemper virus. *Genet Mol Res*, 9, 151-161.
47. Wang, Y., Yu, H., Zhang, J., Gao, J., Ge, X., & Lou, G. (2015). Hesperidin inhibits HeLa cell proliferation through apoptosis mediated by endoplasmic reticulum stress pathways and cell cycle arrest. *BMC cancer*, 15, 1-11.
48. Wudtiwai, B., Makeudom, A., Krisanaprakornkit, S., Pothacharoen, P., & Kongtawelert, P. (2021). Anticancer activities of hesperidin via suppression of up-regulated programmed death-ligand 1 expression in oral cancer cells. *Molecules*, *26*(17), 5345.
49. Mo'men, Y. S., Hussein, R. M., & Kandeil, M. A. (2019). Involvement of PI3K/Akt pathway in the protective effect of hesperidin against a chemically induced liver cancer in rats. *Journal of Biochemical and Molecular Toxicology*, *33*(6), e22305.
50. Yumnam, S., Park, H. S., Kim, M. K., Nagappan, A., Hong, G. E., Lee, H. J., ... & Kim, G. S. (2014). Hesperidin induces paraptosis like cell death in hepatoblatoma, HepG2 cells: Involvement of ERK1/2 MAPK. *PloS one*, *9*(6), e101321.
51. Schreiner, W., Karch, R., Knapp, B., & Ilieva, N. (2012). Relaxation estimation of RMSD in molecular dynamics immunosimulations. *Comput Math Methods Med*, 2012, 173521. https://doi:10.1155/2012/173521

